

Article

Variations of Structural and Functional Traits of *Azolla pinnata* R. Br. in Response to Crude Oil Pollution in Arid Regions

Aya A. Mostafa ¹, Rehab M. Hafez ², Ahmad K. Hegazy ^{2,*}, Azza M. Abd-El Fattah ³, Nermen H. Mohamed ⁴, Yasser M. Mustafa ⁴, Adil A. Gobouri ⁵ and Ehab Azab ^{6,*}

¹ Biotechnology/Bimolecular Chemistry Program, Chemistry Department, Faculty of Science, Cairo University, Giza 12613, Egypt; aamoustafa@sci.cu.edu.eg

² Botany and Microbiology Department, Faculty of Science, Cairo University, Giza 12613, Egypt; rehabhafez@sci.cu.edu.eg

³ Chemistry Department, Faculty of Science, Cairo University, Giza 12613, Egypt; azza682000@yahoo.com

⁴ Egyptian Petroleum Research Institute, Nasr City, Cairo 11727, Egypt; nermenhefny@yahoo.com (N.H.M.); ymoustafa12@yahoo.com (Y.M.M.)

⁵ Department of Chemistry, College of Science, Taif University, Taif 21944, Saudi Arabia; a.gobouri@tu.edu.sa

⁶ Department of Biotechnology, College of Science, Taif University, Taif 21944, Saudi Arabia

* Correspondence: hegazy@sci.cu.edu.eg (A.K.H.); e.azab@tu.edu.sa (E.A.); Tel.: +202-35676651 (A.K.H.)

Abstract: In oil-producing countries, water pollution by crude petroleum oil frequently occurs and causes many environmental problems. This study aims to investigate the effect of crude petroleum oil on the growth and functional traits of the economically important freshwater plant *Azolla pinnata* R. Br. and to report on the plant's resistance to this abiotic stress. Plants were raised in an open greenhouse experiment under different levels of crude oil pollution ranging from 0.5 to 2.0 g/L. Plant functional traits were monitored over a three-week period. Plant cover of *A. pinnata* was decreased with the increased levels of oil pollution. The total chlorophyll content decreased from 0.76 mg/g fresh weight under 2 g/L oil treatment after 21 days of growth. The chlorophyll a/b ratio exceeded the unity at crude oil treatments above 1 g/L, with values reaching 2.78 after seven days, while after 21 days, the ratio ranged from 1.14 to 1.31. The carotenoid content ranged from 0.17 mg/g in the control to 0.11 mg/g in the 2 g/L oil treatment. The carotenoid content varied over time in relation to DNA% damage, which increased from 3.63% in the control to 11.36% in the highest oil treatment level of 2 g/L. The crude oil stress caused severe damage in the frond tissues and chloroplast structure of *A. pinnata*, including a less compacted palisade, the malformation of the epidermis, the disintegration of parenchyma tissue, and the lysis and malformation of the chloroplasts. Since *A. pinnata* cannot withstand high concentrations of crude oil pollution, it is for use in the remediation of slightly polluted freshwaters up to 0.5 g/L.

Keywords: anatomical malformation; chloroplast ultrastructure; pigments; plant cover; genotoxicity



Citation: Mostafa, A.A.; Hafez, R.M.; Hegazy, A.K.; Fattah, A.M.A.-E.; Mohamed, N.H.; Mustafa, Y.M.; Gobouri, A.A.; Azab, E. Variations of Structural and Functional Traits of *Azolla pinnata* R. Br. in Response to Crude Oil Pollution in Arid Regions. *Sustainability* **2021**, *13*, 2142. <https://doi.org/10.3390/su13042142>

Academic Editor: Mohamed A. El-Esawi

Received: 7 January 2021

Accepted: 14 February 2021

Published: 17 February 2021

Publisher's Note: MDPI stays neutral with regard to jurisdictional claims in published maps and institutional affiliations.



Copyright: © 2021 by the authors. Licensee MDPI, Basel, Switzerland. This article is an open access article distributed under the terms and conditions of the Creative Commons Attribution (CC BY) license (<https://creativecommons.org/licenses/by/4.0/>).

1. Introduction

Environmental pollution with crude petroleum oil results from production activities, such as exploration, extraction, and transporting [1,2]. In addition, many accidents occur during production activities, such as drilling, transportation, and leakages from storage tanks and pipelines [1,3]. Crude oil spills in the aquatic ecosystem are exposed to compositional changes in its physical and chemical properties [4,5]. Volatile components are removed by evaporation or oxidized by ultraviolet radiation [6], and low-molecular-weight compounds dissolve in the water [7]. Part of the oil binds to fine suspended particles and settles at the bottom [8] or breaks up into small droplets, forming emulsion dispersed on the water's surface until they decompose [9].

Petroleum hydrocarbons (PHs), particularly the polyaromatic constituents, are the most common persistent organic contaminants in aquatic ecosystems [10]. Their accumulation causes mutagenic toxicity or even death to many living organisms, causing biodiversity

perturbation and loss [11]. Therefore, 16 polycyclic aromatic petroleum oil hydrocarbons are classified as code red pollutants that make remediation a priority for environmental cleanup and human health protection [11].

In the past few decades, different techniques have been applied for the remediation of crude-oil-polluted waters and soils. Among the several biological techniques used are the aquatic macrophytes as an ecologically sound, green technology for the removal of crude petroleum oil pollutants [12–14]. Crude oil consists of a variety of toxic compounds, including hydrocarbons, e.g., alkanes, aromatics, and polycyclic aromatic hydrocarbons and nonhydrocarbons such as sulphur, nitrogen, oxygen, and the metals vanadium, nickel, iron, and copper, which may cause acute and chronic effects on flora, fauna, and human health [5]. The contamination of water bodies with crude oil causes the degradation of aquatic lives. The restoration of degraded ecosystems is extremely difficult and cannot be undertaken without spending extraordinary time and monetary resources.

The conventional clean-up/remediation techniques of oil spills are based on applying physical, mechanical, thermal, and/or chemical methods, with many drawbacks related to their implementation on a large scale. Applications of these methods are expensive, energy-consuming, and environmentally disruptive, and cause negative impacts on ecosystems [5]. Consequently, the use of alternative methods to treat oil-contaminated water bodies is necessary [15]. Phytoremediation as an emerging clean-up technology has numerous advantages over the established engineering remediating techniques [16]. These advantages are summarized in the low cost [14], remediation efficiency [14,17], and lower environmental risk than the conventional methods [14].

The potential use of *Azolla pinnata* for the remediation of crude oil pollution is advantageous for the assessment or removal of inorganic and organic pollutants from water [12,15,16,18,19]. The characteristics of *A. pinnata* include a fast growth rate, pollutant absorption efficiency, low operation cost, and continuous renewability [20]. This species is able to duplicate its biomass within two to three days, forming a condensed mat floating on the water's surface, with each frond acting as a phytoremediator unit, leading to fast and effective reclamation [21]. These characteristics nominate the species to be considered as a green technology for the phytoremediation of polluted waters.

The objectives of this study were to monitor the effect of crude petroleum oil on the growth and functional traits of *Azolla pinnata* R. Br., to report on the plant's resistance to this abiotic stress and to demonstrate its possible role in the phytodegradation of polluted water.

2. Materials and Methods

2.1. Study Species

Azolla pinnata R. Br. (Azollaceae) is a floating aquatic fern native to much of Asia, Africa, and parts of Australia. This fern has a symbiotic relationship with *Anabaena azollae* Strasbur, a nitrogen-fixing Cyanobacterium. The species was introduced in Egypt as an exotic species in the early nineties of the last century as green manure in rice fields before its escape to quiet, slow-moving irrigation and drain canals [3,20,22]. At optimum growth conditions, the plant doubles its biomass within a week. The plant material was obtained from Agric. Microbial Department, Soils, Water and Environment Research Institute (SWERI), Agricultural Research Center (ARC), Giza, Egypt.

The growth water medium was collected from the River Nile in Giza. The crude petroleum oil was obtained from the Asal oil field in Ras-Sidr, West Sinai, Egypt. The chemical composition of the crude oil was shown in our previous publication [10].

2.2. Acclimation and Growth Conditions of *Azolla Pinnata*

To make sure of the appropriate weather conditions for *A. pinnata* growth in the open greenhouse where the experimental treatment was performed, *A. pinnata* was raised for one week in freshwater medium supplemented by freshly prepared Yoshida nutrient solution [23]. The components were prepared using the River Nile water, constituting 0.5 g/L from each of K_2SO_4 , $CaCl_2$, K_2HPO_4 , and $MgSO_4$, and 0.25 g/L of $(NH_4)_2SO_4$. After

the one-week acclimation period, the experimental treatment was conducted in an open greenhouse in the Faculty of Science, Cairo University, during July–August 2018. During the three-week experimental time, the measured minimum–maximum temperatures were 23–34 °C, with day temperature ranging between 26 and 34 °C and a night temperature of 14–21 °C. The daylight hours were 12 h sunshine. The daily relative air humidity ranged between 48 and 66%.

2.3. Petroleum Oil Pollution Treatment

The experiment was performed in glass bowls of 25 cm diameter and 12 cm depth. The outer sides of the bowls were painted dark to prevent the possible growth of algae on the inner sides. To keep the oxygen level in the water, a hydroponic, multinozzle air pump system was used with an airline rubber tube for every bowl. The pumps were adjusted to allow the flow of constant and slow air bubble travel in the bowl. The air flow rate was 5.833×10^{-5} cubic meters per second (m^3/s).

The experiment started in mid-July 2018. One and half liters of freshwater with the nutrient solution was placed in every bowl. The crude petroleum oil treatment was applied at the rates of 0.5, 1.0, 1.5 and 2.0 g/L in three replications, with two controls, a negative control (*Azolla* in water without oil treatment) and a positive control (water and oil treatment without *Azolla*). The oil was mixed in water as suspensions. About 150 g of *A. pinnata* acclimated fern was blotted on towel paper. Four grams of the blotted fern was placed in every bowl. The air pump system was turned on and the experiment was monitored for three weeks. The water levels in the bowls were kept stable through the course of the experiment by freshwater compensation of the evaporated water every other day.

At the end of the three-week experimental time, we assessed the plant functional traits represented by plant cover, photosynthetic pigments, and genotoxicity as DNA% in the comet tail, frond anatomy, and chloroplast structure.

2.4. Plant Cover

The plant cover was determined as the percentage of the growth bowl surface area, which was determined by the dot grid method. The frond cover percentage was calculated according to [24], i.e., frond cover (%) = (area covered by the plant/bowl surface area) \times 100.

2.5. Photosynthetic Pigments

Chlorophyll and carotenoid contents were measured following Hiscox and Tsraelstam (1979) [25]. Two grams of fresh *A. pinnata* samples was placed in a 25 mL stoppered dark tube containing 15 mL concentrated dimethyl sulphoxide (DMSO) and frozen at 4 °C in the laboratory fridge. After thawing, the tissues were macerated and the pigment extract was filtered in dim light through a sintered glass filter, then the filtrate volume was brought to an exact 25 mL volume. The optical density was measured spectrophotometrically with a UV-visible spectrophotometer (Shimadzu UV–1208 model; Canby, OR, USA) at 436, 440, 474, 644 and 662 nm. Pure dimethyl sulfoxide (DMSO) was used as the blank. Measurements were taken in three replications. The chlorophyll and carotenoid contents were calculated as mg per gram fresh weight according to the following equations:

$$\text{Chl a} = [0.0127 A_{622} + 0.02269 A_{644}] \times \text{Dilution factor (mg/g)} \quad (1)$$

$$\text{Chl b} = [0.0229 A_{622} + 0.00468 A_{644}] \times \text{Dilution factor (mg/g)} \quad (2)$$

$$\text{Total Chl} = [0.0202 A_{622} + 0.00802 A_{644}] \times \text{Dilution factor (mg/g)} \quad (3)$$

$$\text{Cx} + \text{c} = [(1000A_{474} - 1.29 \text{ Chl a} - 53.77 \text{ Chl b})/220] \times \text{Dilution factor (mg/g)} \quad (4)$$

where Chl a = chlorophyll a, Chl b = chlorophyll b, Chl a + Chl b = total chlorophyll, Cx + c = carotenoids, and Ax = absorbance at x nm.

2.6. Genotoxic Effects of Crude Petroleum Oil

The genotoxic effect of crude petroleum oil on *A. pinnata* was assessed as DNA damage percentage in the comet tail using an alkaline comet assay (pH > 13) following Tice (2000) [26]. The DNA damage was assessed in *A. pinnata* plants treated with different crude oil levels (0.5, 1, 1.5 and 2 g/L) and compared to nucleic damages in the fronds of the control. Samples of 1 g fresh-weight were gently homogenized in 1 mL of cold mincing solution, releasing the nuclei for analysis. The mincing solution was composed of Hanks' balanced Salt Solution (HBSS) free from calcium and magnesium cations, which was supplemented with 10% (DMSO) and 20 mM ethylene diamine tetra acetic acid (EDTA). The homogenate was filtered to remove the tissue debris.

Then, aliquots of 10 μ L of cell suspension each containing about 10,000 cells mixed with 75 μ L of the low melting point agarose with a concentration of 0.5% *w/v* were evenly mounted on a frosted, clean, glass slide and left until agarose solidification. The slides were incubated for 24 h in chilled lysis buffer in the dark at 4 °C. The lysis buffer (pH 10) consisted of 10 mM Tris, 2.5 M NaCl, and 100 mM EDTA and was freshly supplemented with 1% Triton X-100 and 10% DMSO. Then, the slides were incubated for 20 min in freshly prepared alkaline buffer (pH 13) consisting of 1 mM EDTA and 300 mM NaOH. At this time, the electrophoresis of the uncoiled DNA was conducted at 25 V (0.90 V/cm) and 300 mA for 20 min. Next, the neutralization of the nucleic acid products was performed using 0.4 M Trizma base. The nucleic acid products were fixed in chilled absolute ethanol and air-dried. The DNA damage level was assessed as the amount of DNA fragments that migrated away from the nucleus, expressed as DNA% in the comet tail. This assessment depended on imaging of 50 cells stained with ethidium bromide at 400 \times magnification using Komet 5 image analysis software established by Kinetic Imaging, Ltd (Liverpool, UK).

2.7. Plant Anatomy and Chloroplast Structure

From three petroleum pollution levels (control, 0.5, and 2 g/L), the fronds were collected and rinsed with distilled water, then fixed in 0.1 M Na-cacodylate buffer (pH 7.2) containing 2% ice-cold glutaraldehyde for 4 h following Williams and Carter (1996). The fronds were embedded in blocks of epoxy resin and incubated at 60 °C in an oven overnight before cooling to room temperature. The blocks were sectioned at 100–1000 μ m thickness and stained with 1 X toluidine blue dye according to Bozzola and Russell (1999) [27]. The sections were examined by light microscope (Leica DM750) and photographed by Digital Camera (Leica ICC50 HD). The ultrathin sections (100 μ m thickness) were investigated for chloroplast ultrastructure following Jakstys' method (1999) [27]. Ultrathin sections were stained with uranyl acetate and lead citrate, then were examined by transmission electron microscope (JEOL, JEM-1400). The photographs were captured by a charge-coupled device CCD camera (model AMT).

2.8. Statistical Analysis

The experimental data were obtained in three replications. The results were expressed as mean \pm SE (standard error). Statistical analysis was employed by using the Statistical Package for Social Sciences (SPSS 18.0 for Windows). For comparison among the different treatments in different periods, two-way analysis of variance (ANOVA) and Duncan's multiple range test ($p < 0.05$) were used. The normality assumption was tested with the Shapiro–Wilk test.

3. Results

3.1. Plant Cover

The plant cover of *Azolla pinnata* after a seven day growth period decreased from $97.7 \pm 1.2\%$ ($p < 0.05$) in the control to $87.6 \pm 0.4\%$ and $64.2 \pm 2.7\%$ in the 0.5 and 2 g/L treatments, respectively (Figure 1a,b). A similar trend was observed after 14 and 21 days of growth, with the average plant cover percentage reducing from $100 \pm 0.0\%$ in the control treatment to $92.1 \pm 0.4\%$ in the 0.5 g/L treatment and to $46.6 \pm 2.8\%$ in the

2 g/L treatments after 14 days. The lowest plant cover percentage under different oil treatment concentrations was found after 21 days, with values decreasing to $86.9 \pm 2.6\%$ and $32.6 \pm 0.0\%$ in the 0.5 and 2 g/L treatments, respectively.

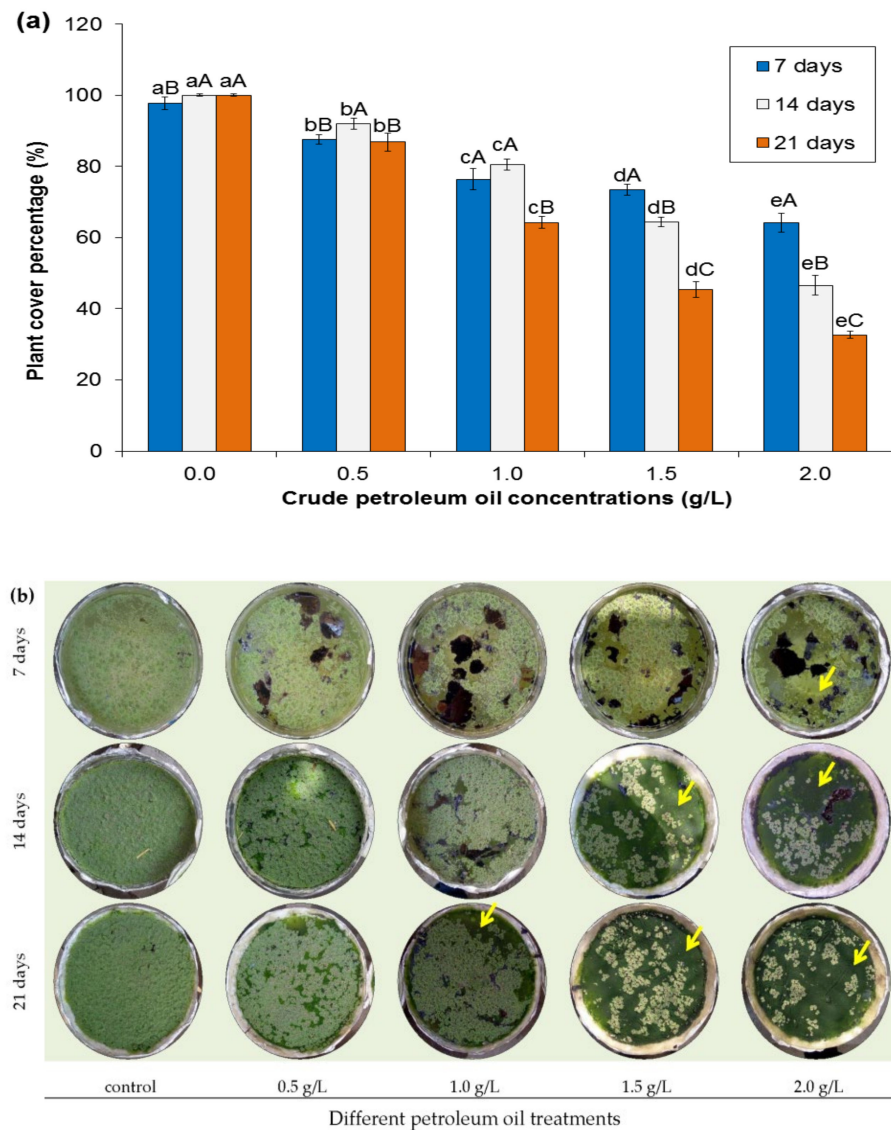


Figure 1. Concentration-dependent effects of crude petroleum oil on plant cover % of *A. pinnata* during three growth periods of 7, 14, and 21 days (a). Representative photographs of *A. pinnata* in the growth containers under different petroleum oil treatments during the three growth periods of 7, 14 and 21 days (b); the yellow arrows in some photos point to the growth of *Anabaena azollae*, the symbiotic cyanobacterium. Different lowercase letters indicate significant differences between different treatments at $p \leq 0.05$, and different capital letters indicate significant differences between the different growth times at each treatment at $p \leq 0.05$. The cover percentage is represented as mean \pm SE.

3.2. Chlorophyll Content

The total chlorophyll content attained the highest values in the control treatment, amounting to 0.4 ± 0.002 , 0.6 ± 0.004 , and 0.8 ± 0.008 mg/g fresh tissues ($p < 0.05$) after 7, 14, and 21 days, respectively (Figure 2). The values decreased with the increase in crude oil concentrations to 0.1 ± 0.004 , 0.49 ± 0.002 , and 0.47 ± 0.02 mg/g in the 2 g/L treatments after 7, 14, and 21 days, respectively.

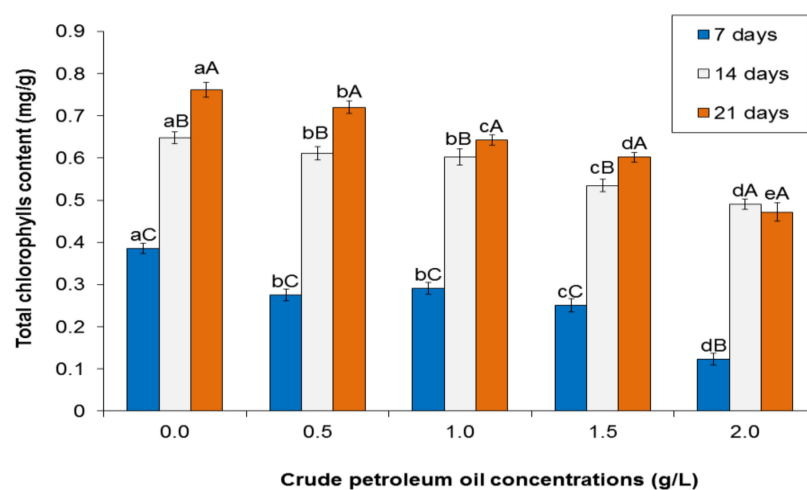


Figure 2. Effects of different petroleum oil concentrations on the total chlorophyll content (mg pigment/g fresh tissue) of *A. pinnata* at three growth time intervals of 7, 14, and 21 days. Different lowercase letters indicate significant differences between different treatments at $p \leq 0.05$, and different capital letters indicate significant differences between the different growth times at each treatment at $p \leq 0.05$. Values are expressed as mean \pm SE.

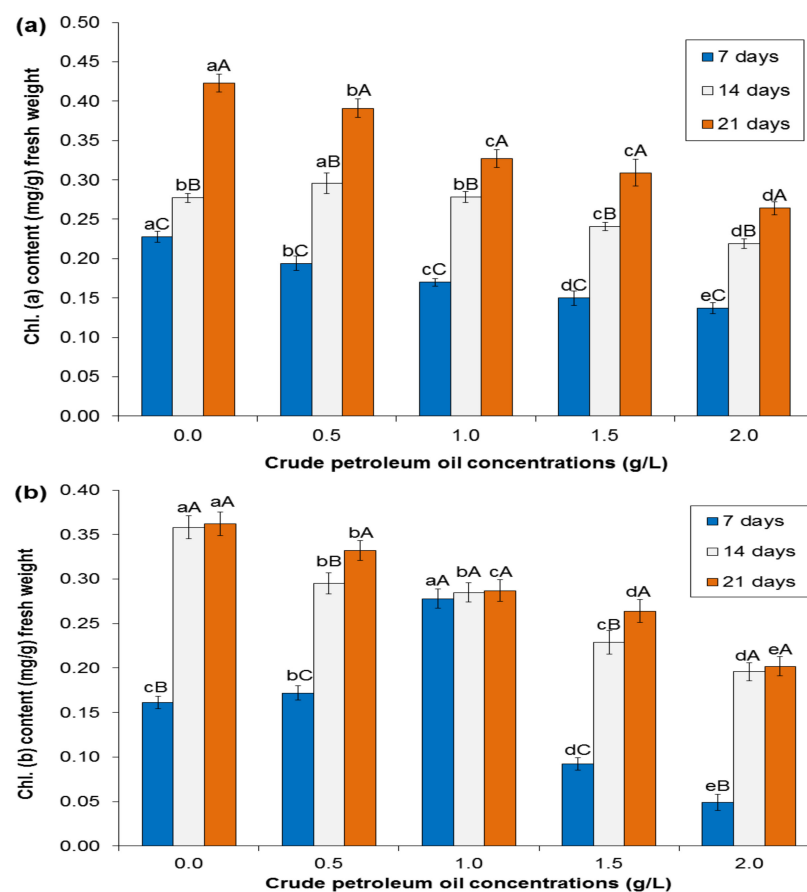


Figure 3. Effects of different petroleum oil concentrations on chlorophyll a content (a) and chlorophyll b content (b) of *A. pinnata* (mg/g fresh tissue) during the three growth periods of 7, 14, and 21 days. Different lowercase letters indicate significant differences between different treatments at $p \leq 0.05$, and different capital letters indicate significant differences between the different growth times at each treatment at $p \leq 0.05$. Chlorophyll contents (a and b) in each treatment are expressed as mean \pm SE.

The chlorophyll a and b contents of *A. pinnata* fronds varied among the different crude oil treatment concentrations and the change in experimental time periods. The values decreased from the control treatment with increasing crude oil concentrations from 0.5 to 2 g/L (Figure 3a,b).

After seven days, chl a and chl b contents under crude oil treatments 1.5 and 2 g/L attained significantly lower values ($p < 0.05$) than the control (Figure 3a,b). The chl a contents decreased from 0.23 ± 0.002 in the control to 0.15 ± 0.009 and 0.14 ± 0.001 mg/g fresh tissues under the 1.5 to 2 g/L crude oil treatments. Similarly, for chl b, the values decreased from 0.16 ± 0.001 to 0.09 ± 0.007 and 0.05 ± 0.006 mg/g fresh tissues, respectively. After 14 and 21 days of growth, the chl a and b contents varied between values higher or lower than the values measured in the control samples, particularly at the crude oil treatments of 1, 1.5, and 2 g/L (Figure 3a,b). At this experimental time, the *A. pinnata* plants showed symptoms of die-back, and the growth of the cyanobacterium *Anabaena azollae* filaments dominated on the water's surface (Figure 1a,b), which appeared on the water's surface as a condensed green matt in only the crude oil treatments, compared with the positive controls, in which the green filament bloom was not observed during the experimental time course.

The chlorophyll a/b ratio was larger than unity in all treatments under the three experimental growth periods, except in the 1 g/L treatment after 7 and 14 days and the negative control after 14 days. The high chl a/b ratios ranged between 1.004 and 2.78 at 0.5 g/L after 14 days and 2 g/L after 7 days, respectively (Figure 4). After 21 days, the chl a/b ratio was higher than after 14 days in all crude oil treatments, with values ranging from 1.1 to 1.3. The lowest chl a/b ratio was 0.61 in 1 g/L after seven days of growth.

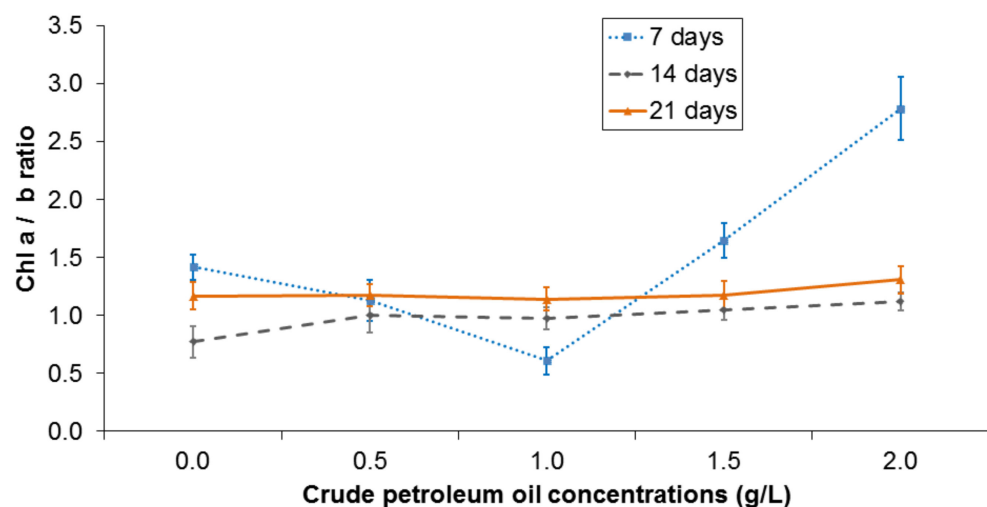


Figure 4. The effect of different petroleum oil concentrations on chl a/b ratio of *A. pinnata* during the three growth periods of 7, 14, and 21 days. Chl a/b ratio in each treatment is expressed as mean \pm SE.

3.3. Carotenoid Content and Comet Image

The carotenoid content, as a nonenzymatic antioxidant, and the oxidative stress inferred by DNA% in the comet tail in response to crude petroleum oil pollution showed significant variations over time (Figures 5a and 6).

After seven days (Figure 5b), the carotenoid content attained the lowest values, ranging from 0.17 ± 0.001 in the control to 0.11 ± 0.003 mg/g fresh tissues at the 2 g/L crude oil treatment in a concentration-dependent manner. Alternatively, the average DNA% in the comet tail significantly increased from 3.6 ± 0.2 in the control treatment to 11.4 ± 0.2 in the highest oil treatment concentration of 2 g/L (Figures 5a and 6).

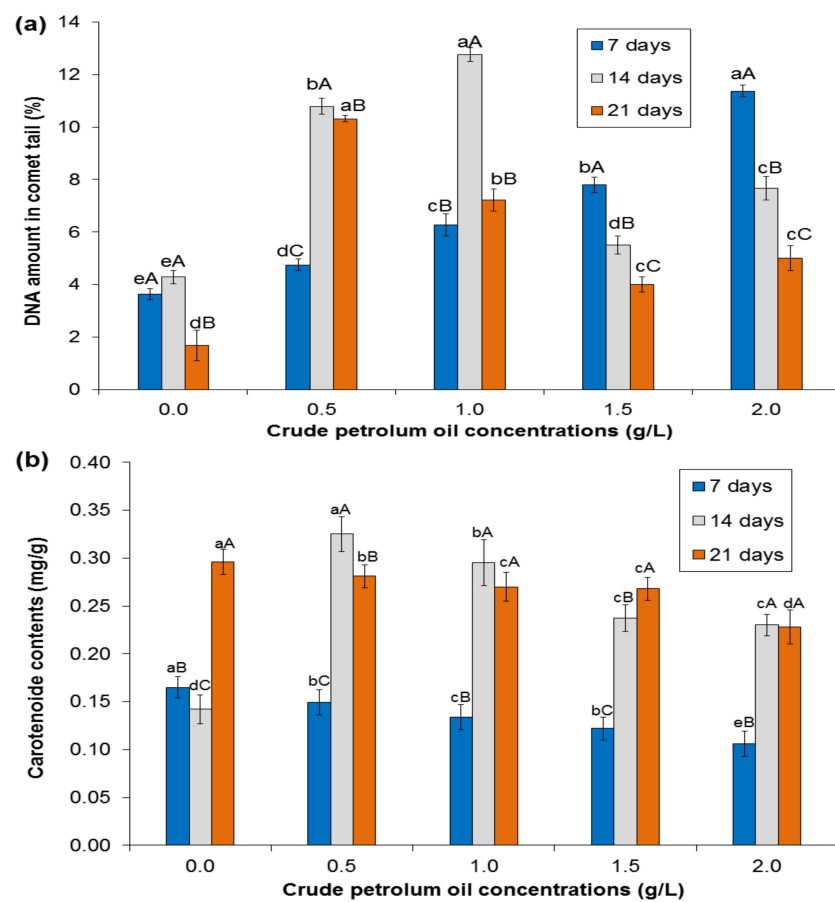


Figure 5. Oxidative damage expressed as DNA% in comet tail assay (a) and carotenoid content (mg/g fresh tissues) (b) of *A. pinnata* after 7 (a), 14 (b), and 21 (c) days under different petroleum oil concentrations versus control. Different lowercase letters indicate significant differences between different treatments at $p \leq 0.05$, and different capital letters indicate significant differences between the different growth times at each treatment at $p \leq 0.05$. The values are expressed as mean \pm SE.

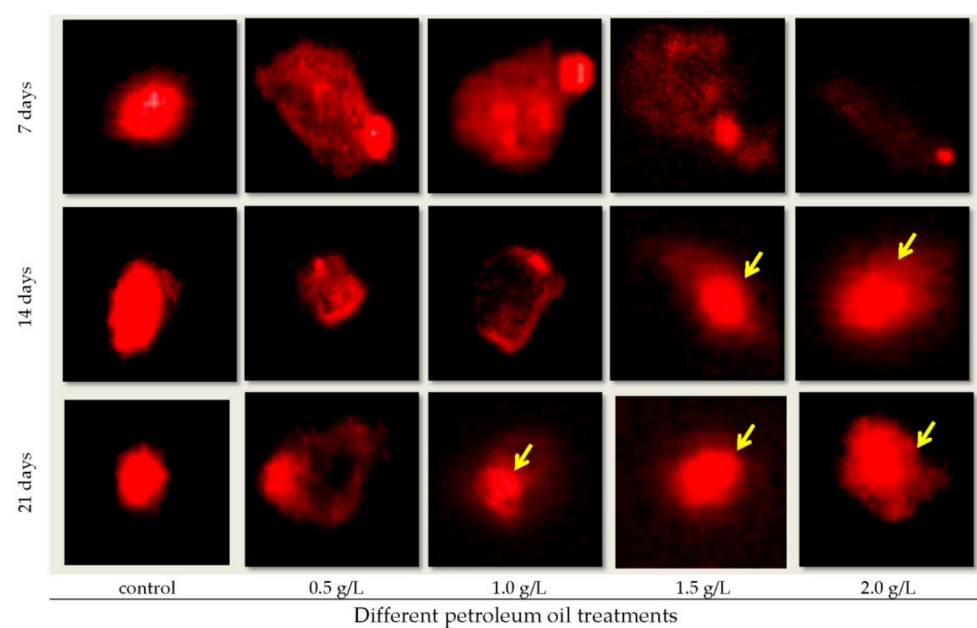


Figure 6. The genotoxicity of crude petroleum oil as shown in comet images of *A. pinnata* plants treated with different petroleum oil treatments after 7, 14, and 21 days. The arrows in some images indicate the almost intact region of the nuclei.

The highest value of carotenoid content after 14 days reached 0.3 ± 0.01 mg/g fresh tissues at 0.5 g/L and gradually reduced to 0.2 ± 0.001 mg/g fresh tissues at 2 g/L (Figure 5b). The DNA% damage after 14 days at 0.5 g/L amounted to $10.8 \pm 0.2\%$, which was significantly higher than the values estimated at 1.5 and 2 g/L, which attained $5.5 \pm 0.005\%$ and $7.7 \pm 1.2\%$, respectively (Figures 5a and 6).

The average carotenoid content after three weeks reduced from 0.3 ± 0.003 mg/g fresh tissues in the control to 0.2 ± 0.008 mg/g fresh tissues at 2 g/L (Figure 5b). The DNA% damage at 0.5 g/L reached $10.3 \pm 0.1\%$, which was significantly higher than the values amounting to 7.2 ± 0.9 , 4 ± 0.5 , and $5 \pm 0.8\%$ in the 1, 1.5, and 2 g/L oil treatments, respectively (Figures 5a and 6).

3.4. Anatomical Structure of the Frond

The light microscope micrographs of the *A. pinnata* frond demonstrated the impact of crude petroleum oil pollution on the anatomical structure (Figure 7). In the control specimen, the frond cavity appeared ellipsoid and lined with one layer of circular adaxial epidermal cells. Close to the adaxial cell layer, the cavity hair cells appeared rounded, similar to air bubbles. The cavity contained the natural endosymbiont microcosm composed of *Anabaena azollae* and different types of bacteria. This microcosm occupied the peripheral region of the cavity laying on the adaxial epidermis, especially around the hair cells, leaving the central area of the cavity empty or filled with liquid or gas. The microcosm population was still located in the peripheral regions of the cavity with increased density throughout the growth periods from 7 to 14 and 21 days. The adaxial epidermis was followed by one layer of palisade parenchyma that consisted of rounded cells, appearing with densely stained cell walls (Figure 7, pictures 1, 4, and 7).

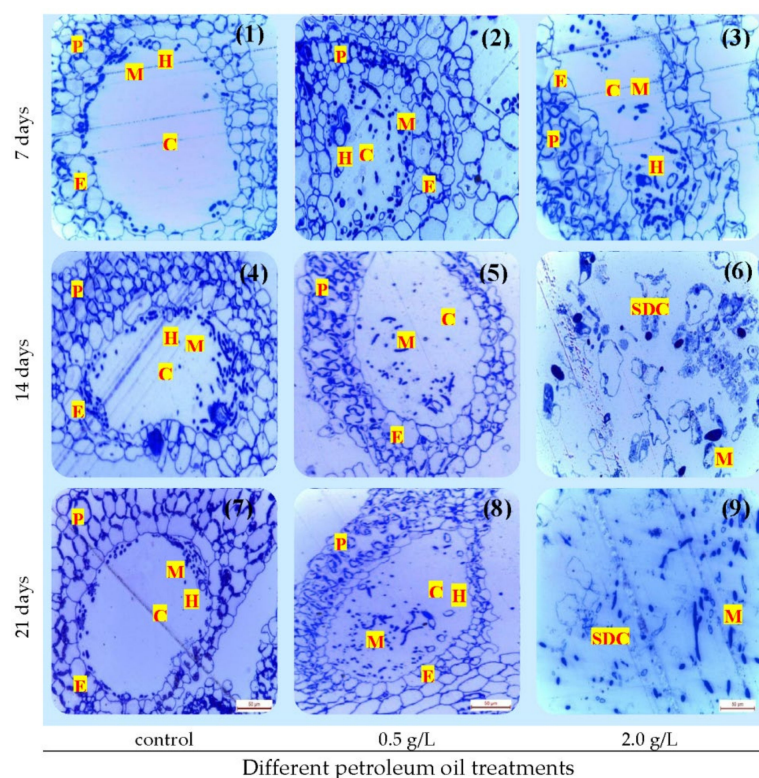


Figure 7. Light micrographs ($40\times$ and scale bar = $50\ \mu\text{m}$) of longitudinal sections of leaf cavities in dorsal lobes of mature fronds of *A. pinnata* treated with different crude petroleum oil concentrations, 0 (control), 0.5, and 2 g/L, raised for three time intervals of 7, 14, and 21 days. The capital letters correspond to different structures of the frond cavity. (C) Frond cavity, (E) adaxial epidermis, (H) hair cell or trichome, (M) microcosm *Anabaena azollae*, (P) palisade tissue, and (SDC) separated deformed cells.

In the 0.5 g/L oil treatment (Figure 7, pictures 2, 5, and 8), the adaxial epidermis appeared integral with the corresponding controls throughout the three-week growth period. In contrast, the palisade tissues became less compacted after the 14- and 21-day growth periods. At 2 g/L, throughout the experimental time course (Figure 7, pictures 3, 6, and 9), a significant malformation of both the adaxial epidermis and the palisade parenchyma ranged from less compacted, as shown in the 0.5 g/L treatment, to completely disintegrated at 14 and 21 days.

The hair cells and the associated microcosm appeared dispersed from the peripheral region of the cavity and invaded the cavity central area at 0.5 g/L and 2 g/L during the experimental time intervals.

3.5. The Ultrastructure of Frond Chloroplasts

In the control, after seven days of growth, the shape and ultrastructure of the chloroplast appeared normal (Figure 8). The chloroplast appeared to have an oval to ellipsoid shape. The thylakoid membranes appeared as dark packages parallel to each other and evenly distributed in the stroma. The starch grains appeared as bright, round or ellipsoid objects. The plastoglobuli appeared as dark, round particles either connected to the stromal interface of the thylakoid membranes or dispersed freely in the stroma.

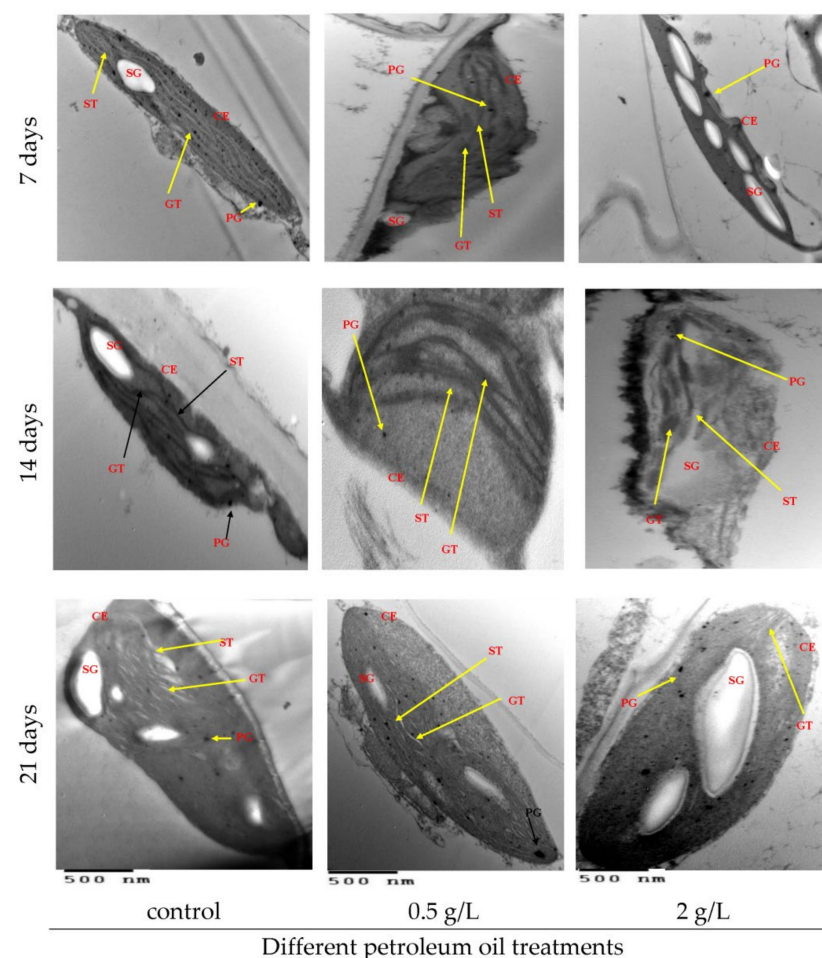


Figure 8. Transmission electron micrographs (bar scale = 500 nm) of chloroplast in palisade tissue of mature fronds of *A. pinnata* raised under different crude petroleum oil concentrations of 0 (control), 0.5, and 2 g/L for three time intervals of 7, 14, and 21 days. The capital letters correspond to different structures of the chloroplast. (CE) chloroplast envelope, (GT) grana thylakoids, (PG) plastoglobuli, (SG) starch grains, and (ST) stroma thylakoids.

The shape and functional ultrastructure of the chloroplast after 14 and 21 days demonstrated significant malformations in the control and at the 0.5 g/L and 2 g/L oil treatments. The chloroplast shape appeared elongated, rounded, or arched and swollen at the 0.5 g/L and 2 g/L oil treatments. The lysis of the chloroplast envelope was observed at 2 g/L. The thylakoid membrane arrangements varied between the different oil treatments where the grana and the stroma thylakoid membranes disappeared from the stroma of the chloroplasts. The thylakoid network became loose, resulting in its appearance as separated dark patches.

The number and size of starch grains in chloroplast stroma were variable in the oil treatments compared with the control (Figure 8). At 0.5 g/L after 7 and 14 days, the starch grains appeared faint or smaller in size than in the control sample and in the 0.5 g/L oil treatment after 21 days. Alternatively, the number of starch grains increased in the controls after 14 and 21 days in the 2 g/L oil treatment. The plastoglobuli appeared larger in size at both 0.5 g/L and 2 g/L in all oil treatments after the three time intervals of 7, 14, and 21 days.

4. Discussion

This study attempted to monitor the effects of crude petroleum oil on the growth and functional trails of *Azolla pinnata* as indicators for plant resistance to this abiotic stress, and to report on its possible role in the phytodegradation of crude oil in polluted water.

The death of *A. pinnata* under higher petroleum oil concentrations may be related to perturbations of photosynthetic pigments due to their critical role in plant growth [28]. Other studies proved the phytotoxic effects of petroleum oil on photosynthesis [29,30], where plants resorted to changing their chlorophyll content to adapt to different environmental conditions. The decreased plant cover of *A. pinnata* with increasing oil treatment from 0.5 g/L to 2 g/L over the three-week growth period seemed to be consistent with the study on *Azolla pinnata* under different diesel concentrations [31]. Generally, the reduction in total chlorophyll content with the increased oil treatment may enhance chlorophyll degradation via the oxidative stress induced by petroleum pollution [32].

Since chl a and chl b are necessary for the primary reaction in photosynthesis, the chl a/b ratio indicates the plant's capacity to carry out photosynthesis [30,33]. Chl a/b ratios lower than unity indicate a reduction in chl a and increased chl b, which is considered to be a trade-off between the chlorophylls, where chlorophyll b is characterized by harvesting a wider range of light due to its different absorption spectrum from that of chlorophyll a [34,35]. Other studies showed a chl a reduction in response to abiotic stress, including petroleum oil pollution [29,30]. The increased content of chl b due to petroleum oil pollution was reported in other studies [30,36,37]. Generally, the decreased chlorophyll content in response to increased levels of crude petroleum oil pollution is attributed to chlorophyll degradation due to oxidative damage, resulting in the induction of leaf senescence [38,39]. Carotenoids represent potential nonenzymatic antioxidant biomolecules [40,41]. Carotenoids are important for plants to mitigate the oxidative stress induced by many environmental stresses, including petroleum hydrocarbon pollution via free-radical scavenging [42,43]. Carotenoids preserve cellular structures and biomolecules, including DNA, from oxidative damage [44,45]. The petroleum oil concentrations caused a reduction in carotenoid content after seven days, similarly to other plants under petroleum pollution [46,47]. Such reductions may be due to oxidation by reactive oxygen species produced under the abiotic stresses [46]. Our study demonstrated an inverse relationship between DNA damage and carotenoid content, similar to the results of other studies [46].

The reduction in DNA damage was accompanied by the reduction in carotenoid content in *A. pinnata* fronds at higher pollution levels of 1.5 and 2 g/L after 14 days and in the 1 and 2 g/L treatments after 21 days. These results may be attributed to the induction of DNA repair by secretions of *A. azollae* that formed condensed green mats at pollution levels 1.5 and 2 g/L after 14 days and in the 1 and 2 g/L treatments after 21 days. The

cyanobacterium *A. azollae* secretes exopolysaccharides (RPS), which were released freely into the growth medium of *A. pinnata* [48,49]. The RPS of different genera of cyanobacteria, including *Anabaena*, exhibit antioxidant and scavenging activities against reactive oxygen species [49]. As antioxidant compounds, RPS of *A. azollae* have the potential to repair damaged biomolecules, including nucleic acids [50,51]. Therefore, we infer that RPS of *A. azollae* may be responsible for repairing DNA damage in *A. pinnata* under high oil pollution levels associated with low frond carotenoid contents. The intensive growth of *A. azollae* at higher pollution levels was similar to the behavior of the cyanobacterium *Anabaena variabilis*, which has the ability to bloom at high petroleum oil pollutions for a long time [52].

The anatomical peculiarities demonstrated that both high crude petroleum oil concentrations (2 g/L) and longer exposure periods (21 days) disrupted the symbiotic relationship between *A. pinnata* and its N₂-fixing endophyte *A. azollae* by the deformation of the cavity hair cells or trichomes and fern packet rupture [53,54]. The cavity hair cells play a critical role in nitrogen fixation supplementation to the fern [55]. *A. azollae* filaments were released from the damaged frond cavity into the water medium, forming condensed green mats on the water surface due to its photosynthetic activity and nitrogen-fixating performances [20].

As a result of the disruption of the symbiosis between the fern and cyanobacterium partners of *A. pinnata* due to petroleum oil water pollution, we inferred that *A. pinnata* suffered from nitrogen starvation. Many studies proved that nitrogen starvation has a negative effect on plant growth through photosynthesis perturbations [39,56,57]. For instance, leaf senescence was observed with elevations of reactive oxygen species (ROS), resulting in photosynthetic protein degradation and chloroplast structural damage appearing as chloroplast malformation and thylakoid membrane disintegration. The reduction in photosynthetic activity was accompanied by a significant reduction in soluble sugar contents as the main product of photosynthesis, which are essential for biological processes [58]. For the plant to mitigate the malfunction of the chloroplasts, an alternative pathway may be established to supply the plant with sufficient amounts of soluble sugars [59]. As appears from the ultrastructure of the chloroplast in our study, it is proposed that the alternative pathway is hydrolysis of the starch grains stored in the chloroplast stroma using chloroplast starch hydrolytic enzymes [59–61]. This assumption depends on the starch grain numbers decreasing or appearing faint at the 0.5 g/L oil treatment after 21 days, or being recorded as absent in the chloroplast stroma at the 0.5 g/L oil treatment after 7 and 14 days. This means that *A. pinnata* resists the reduction in photosynthetic activity under low petroleum oil concentrations.

Other studies reported that the accumulation of starch grains under pollution stress was attributed to the oxidative damage of key player enzymes involved in starch breakdown to the soluble sugars maltose and glucose [59–62]. Additionally, the sugar transporter proteins located in the chloroplast membranes that facilitate the diffusion of maltose and glucose across the inner chloroplast envelope may sustain plant metabolism and growth [58,63]. The increase in size of the plastoglobuli granules under the petroleum oil pollution level of 2 g/L after 21 days of growth seems to be attributed to the high level of pollution stress [64–67]. These stresses induce the dismantling of the thylakoid membrane via lipid peroxidation, leading to the accumulation of degraded lipids in the plastoglobuli hydrophobic core [65].

5. Conclusions

The findings of this study proved that the contamination of freshwater by crude oil adversely affects the functional traits of *A. pinnata*, which negatively affects plant growth and reproduction. The increase in the crude oil pollution from 0.5 to 2 g/L decreased the frond cover by disrupting the photosynthetic activity of the fern. The evidence for the disruption of photosynthesis was apparent in the ultrastructural perturbations of the chloroplast, causing reductions in the total chlorophyll and carotenoid contents. The comet assay results of *A. pinnata* fronds did not show severe genotoxic effects. A possible

explanation of the comet assay results could be due to the intensive growth of *A. azollae*, which may have induced the repair of DNA damage of the fern under crude oil stress. Although the symbiosis between the plant and cyanobiont was disrupted, *Anabaena azollae* was able to adapt more than *Azolla pinnata* under the stressful conditions of the high crude oil pollution levels above 0.5 g/L for 21 days of growth. Therefore, *Azolla pinnata* can be used to remediate low crude oil pollution levels up to 0.5 g/L. Due to the greater durability of *Anabaena azollae* of higher levels of crude oil than *Azolla pinnata*, further studies are recommended to elucidate the phytoremediation efficiency of *A. azollae* of polluted freshwater with high levels of crude oil.

Author Contributions: Conceptualization, A.K.H., R.M.H. and A.A.M.; methodology, A.A.M., R.M.H., A.M.A.-E.F. and E.A.; software, E.A. and A.A.M. and A.A.G.; validation, A.K.H., R.M.H. and A.A.M.; formal analysis, all authors contributed; investigation, A.K.H., R.M.H., A.A.M. and N.H.M.; resources, E.A., Y.M.M., N.H.M. and A.A.G.; data curation, A.A.M., R.M.H. and E.A.; writing—original draft preparation, A.A.M., R.M.H. and A.K.H.; writing—review and editing, A.K.H., R.M.H. and E.A.; visualization, A.K.H., A.A.M. and R.M.H.; supervision, A.K.H., R.M.H. and A.M.A.-E.F.; funding acquisition, A.A.G., A.K.H. and E.A. All authors have read and agreed to the published version of the manuscript.

Funding: This research received no external funding.

Data Availability Statement: The data presented in this study are available on request from the corresponding author.

Acknowledgments: We thank Taif University Researchers Supporting Project number (TURSP-2020/13), Taif University, Taif, Saudi Arabia. We also thank Reda M. El-Shahat, Microbiology Department, Soils; Water and Environment Research Institute, Agriculture Research Center, Giza for the provision of *Azolla pinnata* plant material.

Conflicts of Interest: The authors declare no conflict of interest.

References

1. Eshagberi, G.O. Toxic Effects of Water Soluble Fractions of Crude Oil, Diesel and Gasoline on *Ceratophyllum Demersum*. *Int. J. Health Med.* **2017**, *2*, 2518–0630. [[CrossRef](#)]
2. Margesin, R.; Walder, G.; Schinner, F. Bioremediation Assessment of a BTEX-Contaminated Soil. *Acta Biotechnol.* **2003**, *23*, 29–36. [[CrossRef](#)]
3. Hegazy, A.K.; Diekmann, M.; Ayad, G. Impact of plant invasions on ecosystems and native gene pools. In *Environment 2000 and Beyond*; Hegazy, A.K., Ed.; Horus for Computer and Printing: Cairo, Egypt, 1999.
4. Mendelsohn, I.A.; Andersen, G.L.; Baltz, D.M.; Caffey, R.H.; Carman, K.R.; Fleeger, J.W.; Joye, S.B.; Lin, Q.; Maltby, E.; Overton, E.B.; et al. Oil Impacts on Coastal Wetlands: Implications for the Mississippi River Delta Ecosystem after the Deepwater Horizon Oil Spill. *Bioscience* **2012**, *62*, 562–574. [[CrossRef](#)]
5. Yavari, S.; Malakahmad, A.; Sapari, N.B. A Review on Phytoremediation of Crude Oil Spills. *Water Air Soil Pollut.* **2015**, *226*, 1–18. [[CrossRef](#)]
6. Williams, S.D.; Ladd, D.E.; Farmer, J. *Fate and Transport of Petroleum Hydrocarbons in Soil and Ground Water at Big South Fork National River and Recreation Area, Tennessee and Kentucky, 2002–2003*; US Department of the Interior, US Geological Survey: Washington, DC, USA, 2006; pp. 2005–5104.
7. Venosa, A.D.; Zhu, X. Biodegradation of Crude Oil Contaminating Marine Shorelines and Freshwater Wetlands. *Spill Sci. Technol. Bull.* **2003**, *8*, 163–178. [[CrossRef](#)]
8. Lee, R.F.; Page, D.S. Petroleum hydrocarbons and their effects in subtidal regions after major oil spills. *Mar. Pollut. Bull.* **1997**, *34*, 928–940. [[CrossRef](#)]
9. Kingston, P.F. Long-term Environmental Impact of Oil Spills. *Spill Sci. Technol. Bull.* **2002**, *7*, 53–61. [[CrossRef](#)]
10. Moubasher, H.; Hegazy, A.K.; Mohamed, N.H.; Moustafa, Y.; Kabiell, H.; Hamad, A. Phytoremediation of soils polluted with crude petroleum oil using *Bassia scoparia* and its associated rhizosphere microorganisms. *Int. Biodeterior. Biodegrad.* **2015**, *98*, 113–120. [[CrossRef](#)]
11. Das, K.; Mukherjee, A.K. Crude petroleum-oil biodegradation efficiency of *Bacillus subtilis* and *Pseudomonas aeruginosa* strains isolated from a petroleum-oil contaminated soil from North-East India. *Bioresour. Technol.* **2007**, *98*, 1339–1345. [[CrossRef](#)]
12. Lin, Q.; Mendelsohn, I.A. Evaluation of tolerance limits for restoration and phytoremediation with *Spartina alterniflora* in crude oil-contaminated coastal salt marshes. *Int. Oil Spill Conf. Proc.* **2008**, *2008*, 869–873. [[CrossRef](#)]

13. Ibañez, S.G.; Paisio, C.E.; Wevar Oller, A.L.; Talano, M.A.; González, P.S.; Medina, M.I.; Agostini, E. Overview and new insights of genetically engineered plants for improving phytoremediation. In *Phytoremediation: Management of Environmental Contaminants*; Ansari, A.A., Gill, S.S., Gill, R., Lanza, G.R., Newman, L., Eds.; Springer International Publishing: Cham, Switzerland, 2015; Volume 1.
14. Jan, S.; Parray, J.A. Biodiversity Prospecting for Phytoremediation of Metals in the Environment. In *Approaches to Heavy Metal Tolerance in Plants*; Springer International Publishing: Cham, Switzerland, 2016; pp. 103–110.
15. Kösesakal, T.; Ünlü, V.S.; Külen, O.; Memon, A.; Yuksel, B. Evaluation of the phytoremediation capacity of *Lemna minor* L. in crude oil spiked cultures. *Turk. J. Boil.* **2015**, *39*, 479–484. [[CrossRef](#)]
16. Azab, E.; Hegazy, A.K.; Gobouri, A.A.; Elkesh, A. Impact of Transgenic *Arabidopsis thaliana* Plants on Herbicide Isoproturon Phytoremediation through Expressing Human Cytochrome P450-1A2. *Biology* **2020**, *9*, 362. [[CrossRef](#)]
17. Kebeish, R.; Azab, E.; Peterhaensel, C.; El-Basheer, R. Engineering the metabolism of the phenylurea herbicide chlortoluron in genetically modified *Arabidopsis thaliana* plants expressing the mammalian cytochrome P450 enzyme CYP1A2. *Environ. Sci. Pollut. Res.* **2014**, *21*, 8224–8232. [[CrossRef](#)] [[PubMed](#)]
18. Azab, E.; Hegazy, A.K.; El-Sharnouby, M.E.; ElSalam, H.E.A. Phytoremediation of the organic Xenobiotic simazine by p450-1a2 transgenic *Arabidopsis thaliana* plants. *Int. J. Phytoremediation* **2016**, *18*, 738–746. [[CrossRef](#)]
19. Azab, E.; Kebeish, R.; Hegazy, A. Expression of the human gene CYP1A2 enhances tolerance and detoxification of the phenylurea herbicide linuron in *Arabidopsis thaliana* plants and *Escherichia coli*. *Environ. Pollut.* **2018**, *238*, 281–290. [[CrossRef](#)] [[PubMed](#)]
20. Azab, E.; Soror, A.-F.S. Physiological Behavior of the Aquatic Plant *Azolla* sp. in Response to Organic and Inorganic Fertilizers. *Plants* **2020**, *9*, 924. [[CrossRef](#)]
21. Sood, A.; Uniyal, P.L.; Prasanna, R.; Ahluwalia, A.S. Phytoremediation Potential of Aquatic Macrophyte, *Azolla*. *Ambio* **2011**, *41*, 122–137. [[CrossRef](#)] [[PubMed](#)]
22. Boulos, L. *Flora of Egypt Checklist, Revised Annotated Edition*; Al Hadara Publishing: Cairo, Egypt, 2009.
23. Yoshida, S.; Institute, I.R.R. *Laboratory Manual for Physiological Studies of Rice*; International Rice Research Institute: Los Baños, Philippines, 1976.
24. Zhu, J.; Peng, Z.; Liu, X.; Deng, J.; Zhang, Y.; Hu, W. Response of Aquatic Plants and Water Quality to Large-Scale Nymphaeoides peltata Harvest in a Shallow Lake. *Water* **2019**, *11*, 77. [[CrossRef](#)]
25. Hiscox, J.D.; Israelstam, G.F. A method for the extraction of chlorophyll from leaf tissue without maceration. *Can. J. Bot.* **1979**, *57*, 1332–1334. [[CrossRef](#)]
26. Tice, R.R.; Agurell, E.; Anderson, D.; Burlinson, B.; Hartmann, A.; Kobayashi, H.; Miyamae, Y.; Rojas, E.; Ryu, J.C.; Sasaki, Y.F. Single cell gel/comet assay: Guidelines for in vitro and in vivo genetic toxicology testing. *Environ. Mol. Mutagenes.* **2000**, *35*, 206–221. [[CrossRef](#)]
27. Bozzola, J.J.; Russell, L.D. *Electron Microscopy Principles and Techniques for Biologists*. Available online: <http://search.ebscohost.com/login.aspx?direct=true&scope=site&db=nlebk&db=nlabk&AN=25575> (accessed on 1 March 1991).
28. Baruah, P.; Saikia, R.R.; Baruah, P.P.; Deka, S. Effect of crude oil contamination on the chlorophyll content and morpho-anatomy of *Cyperus brevifolius* (Rottb.) Hassk. *Environ. Sci. Pollut. Res.* **2014**, *21*, 12530–12538. [[CrossRef](#)] [[PubMed](#)]
29. Gilde, K.; Pinckney, J.L. Sublethal Effects of Crude Oil on the Community Structure of Estuarine Phytoplankton. *Chesap. Sci.* **2012**, *35*, 853–861. [[CrossRef](#)]
30. Atta, A.M.; Mohamed, N.H.; Hegazy, A.K.; Moustafa, Y.M.; Mohamed, R.R.; Safwat, G.; Diab, A.A. Green Technology for Remediation of Water Polluted with Petroleum Crude Oil: Using of *Eichhornia crassipes* (Mart.) Solms Combined with Magnetic Nanoparticles Capped with Myrrh Resources of Saudi Arabia. *Nanomaterials* **2020**, *10*, 262. [[CrossRef](#)] [[PubMed](#)]
31. Al-Baldawi, I.A.; Abdullah, S.; Suja, F.; Anuar, N.; Idris, M. Preliminary Test of Hydrocarbon Exposure on *Azolla pinnata* in Phytoremediation Process. Available online: <http://www.ipcbee.com/vol33/047-ICEEB2012-FB015.pdf> (accessed on 10 October 2020).
32. Pokora, W.; Tukaj, Z. The combined effect of anthracene and cadmium on photosynthetic activity of three *Desmodium* (Chlorophyta) species. *Ecotoxicol. Environ. Saf.* **2010**, *73*, 1207–1213. [[CrossRef](#)]
33. Li, Y.; He, N.; Hou, J.; Xu, L.; Liu, C.; Zhang, J.; Wang, Q.; Zhang, X.; Wu, X. Factors Influencing Leaf Chlorophyll Content in Natural Forests at the Biome Scale. *Front. Ecol. Evol.* **2018**, *6*, 6. [[CrossRef](#)]
34. Fahmy, G.M.; Hegazy, A.K.; Hassan, H.T. Phenology, Pigment Content and Diurnal Change of Proline in Green and Senescing Leaves of Three *Zygophyllum* Species. *Flora* **1990**, *184*, 423–436. [[CrossRef](#)]
35. Tanaka, R.; Tanaka, A. Chlorophyll cycle regulates the construction and destruction of the light-harvesting complexes. *Biochim. Biophys. Acta Bioenerg.* **2011**, *1807*, 968–976. [[CrossRef](#)] [[PubMed](#)]
36. Alzurfi, S.K.L.; Alasedi, K.K.; Abdulraheem, N.I. Effect different concentrations of crude oil on the pigment content and protein content of *Hydrilla verticillata* plant. *Iraqi J. Sci.* **2019**, *60*, 2141–2148.
37. Odukoya, J.; Lambert, R.; Sakrabani, R. Impact of Crude Oil on Yield and Phytochemical Composition of Selected Green Leafy Vegetables. *Int. J. Veg. Sci.* **2019**, *25*, 554–570. [[CrossRef](#)]
38. Noori, A.; Maivan, H.Z.; Alaie, E.; Newman, L.A. *Leucanthemum vulgare* lam. crude oil phytoremediation. *Int. J. Phytoremediation* **2018**, *20*, 1292–1299. [[CrossRef](#)] [[PubMed](#)]
39. Zakari, S.A.; Asad, M.-A.-U.; Han, Z.; Zhao, Q.; Cheng, F. Relationship of Nitrogen Deficiency-Induced Leaf Senescence with ROS Generation and ABA Concentration in Rice Flag Leaves. *J. Plant Growth Regul.* **2020**, *39*, 1503–1517. [[CrossRef](#)]

40. Shi, X.; Wu, H.; Shi, J.; Xue, S.J.; Wang, D.; Wang, W.; Cheng, A.; Gong, Z.; Chen, X.; Wang, C. Effect of modifier on the composition and antioxidant activity of carotenoid extracts from pumpkin (*Cucurbita maxima*) by supercritical CO₂. *LWT* **2013**, *51*, 433–440. [[CrossRef](#)]
41. Shen, Y.; Li, J.; Gu, R.; Yue, L.; Wang, H.; Zhan, X.; Xing, B. Carotenoid and superoxide dismutase are the most effective antioxidants participating in ROS scavenging in phenanthrene accumulated wheat leaf. *Chemosphere* **2018**, *197*, 513–525. [[CrossRef](#)] [[PubMed](#)]
42. Farooq, M.A.; Ali, S.; Hameed, A.; Ishaque, W.; Mahmood, K.; Iqbal, Z. Alleviation of cadmium toxicity by silicon is related to elevated photosynthesis, antioxidant enzymes; suppressed cadmium uptake and oxidative stress in cotton. *Ecotoxicol. Environ. Saf.* **2013**, *96*, 242–249. [[CrossRef](#)] [[PubMed](#)]
43. Pilon, C.; Soratto, R.P.; Broetto, F.; Fernandes, A.M. Foliar or Soil Applications of Silicon Alleviate Water-Deficit Stress of Potato Plants. *Agron. J.* **2014**, *106*, 2325–2334. [[CrossRef](#)]
44. Park, J.S.; Chyun, J.H.; Kim, Y.K.; Line, L.L.; Chew, B.P. Astaxanthin decreased oxidative stress and inflammation and enhanced immune response in humans. *Nutr. Metab.* **2010**, *7*, 18. [[CrossRef](#)]
45. Serpeloni, J.M.; Barcelos, G.R.M.; Angeli, J.P.F.; Mercadante, A.Z.; Bianchi, M.L.P.; Antunes, L.M.G. Dietary carotenoid lutein protects against DNA damage and alterations of the redox status induced by cisplatin in human derived HepG2 cells. *Toxicol. Vitro.* **2012**, *26*, 288–294. [[CrossRef](#)]
46. Ben Ghnaya, A.; Charles, G.; Hourmant, A.; Ben Hamida, J.; Branchard, M. Physiological behaviour of four rapeseed cultivar (*Brassica napus* L.) submitted to metal stress. *Comptes Rendus Biol.* **2009**, *332*, 363–370. [[CrossRef](#)]
47. Balliana, A.G.; Moura, B.B.; Inckot, R.C.; Bona, C. Development of *Canavalia ensiformis* in soil contaminated with diesel oil. *Environ. Sci. Pollut. Res.* **2016**, *24*, 979–986. [[CrossRef](#)]
48. Kumar, D.; Kaatánek, P.; Adhikary, S.P. Exopolysaccharides from cyanobacteria and microalgae and their commercial application. *Curr. Sci.* **2018**, *115*, 234. [[CrossRef](#)]
49. Tiwari, O.N.; Mondal, A.; Bhunia, B.; Bandyopadhyay, T.K.; Jaladi, P.; Oinam, G.; Indrama, T. Purification, characterization and biotechnological potential of new exopolysaccharide polymers produced by cyanobacterium *Anabaena* sp. CCC 745. *Polymer* **2019**, *178*, 121695. [[CrossRef](#)]
50. Sikorski, Z.; Kolakowska, A. *Chemical, Biological, and Functional Aspects of Food Lipids*; CRC Press: Boca Raton, FL, USA, 2011; p. 512. [[CrossRef](#)]
51. Skała, E.; Sitarek, P.; Rózsalski, M.; Krajewska, U.; Szemraj, J.; Wysokińska, H.; Śliwiński, T. Antioxidant and DNA Repair Stimulating Effect of Extracts from Transformed and Normal Roots of *Rhaponticum carthamoides* against Induced Oxidative Stress and DNA Damage in CHO Cells. *Oxid. Med. Cell. Longev.* **2016**, *2016*, 1–11. [[CrossRef](#)]
52. Samary Atyah, B.; Al-Mayaly, I.K.A. Biodegradation of Crude Oil by *Anabaena variabilis* Isolated from Al-Dora Refinery. *J. Pharm. Biol. Sci.* **2018**, *13*, 51–56.
53. Burritt, D.J. The polycyclic aromatic hydrocarbon phenanthrene causes oxidative stress and alters polyamine metabolism in the aquatic liverwort *Riccia fluitans* L. *Plant Cell Environ.* **2008**, *31*, 1416–1431. [[CrossRef](#)] [[PubMed](#)]
54. Liu, H.; Weisman, D.; Ye, Y.-B.; Cui, B.; Huang, Y.-H.; Colón-Carmona, A.; Wang, Z.-H. An oxidative stress response to polycyclic aromatic hydrocarbon exposure is rapid and complex in *Arabidopsis thaliana*. *Plant Sci.* **2009**, *176*, 375–382. [[CrossRef](#)]
55. Uheda, E.; Maejima, K.; Shiomi, N. Localization of Glutamine Synthetase Isoforms in Hair Cells of *Azolla* Leaves. *Plant Cell Physiol.* **2004**, *45*, 1087–1092. [[CrossRef](#)]
56. Oka, M.; Shimoda, Y.; Sato, N.; Inoue, J.; Yamazaki, T.; Shimomura, N.; Fujiyama, H. Abscisic acid substantially inhibits senescence of cucumber plants (*Cucumis sativus*) grown under low nitrogen conditions. *J. Plant Physiol.* **2012**, *169*, 789–796. [[CrossRef](#)]
57. Meng, S.; Peng, J.-S.; He, Y.-N.; Zhang, G.-B.; Yi, H.-Y.; Fu, Y.-L.; Gong, J.-M. *Arabidopsis* NRT1.5 Mediates the Suppression of Nitrate Starvation-Induced Leaf Senescence by Modulating Foliar Potassium Level. *Mol. Plant* **2016**, *9*, 461–470. [[CrossRef](#)]
58. Niittylä, T.; Messerli, G.; Trevisan, M.; Chen, J.; Smith, A.M.; Zeeman, S.C. A Previously Unknown Maltose Transporter Essential for Starch Degradation in Leaves. *Science* **2004**, *303*, 87–89. [[CrossRef](#)]
59. Yu, T.-S.; Kofler, H.; Häusler, R.E.; Hille, D.; Flügge, U.-I.; Zeeman, S.C.; Smith, A.M.; Kossmann, J.; Lloyd, J.; Ritte, G.; et al. The *Arabidopsis* *sex1* Mutant Is Defective in the R1 Protein, a General Regulator of Starch Degradation in Plants, and Not in the Chloroplast Hexose Transporter. *Plant Cell* **2001**, *13*, 1907–1918. [[CrossRef](#)]
60. Edner, C.; Li, J.; Albrecht, T.; Mahlow, S.; Hejazi, M.; Hussain, H.; Kaplan, F.; Guy, C.; Smith, S.M.; Steup, M.; et al. Glucan, Water Dikinase Activity Stimulates Breakdown of Starch Granules by Plastidial β -Amylases. *Plant Physiol.* **2007**, *145*, 17–28. [[CrossRef](#)] [[PubMed](#)]
61. Hejazi, M.; Fettke, J.; Haebel, S.; Edner, C.; Paris, O.; Frohberg, C.; Steup, M.; Ritte, G. Glucan, water dikinase phosphorylates crystalline maltodextrins and thereby initiates solubilization. *Plant J.* **2008**, *55*, 323–334. [[CrossRef](#)] [[PubMed](#)]
62. Zeeman, S.C.; Delatte, T.; Messerli, G.; Umhang, M.; Stettler, M.; Mettler, T.; Streb, S.; Reinhold, H.; Kötting, O. Starch breakdown: Recent discoveries suggest distinct pathways and novel mechanisms. *Funct. Plant Biol.* **2007**, *34*, 465–473. [[CrossRef](#)]
63. Stettler, M.; Eicke, S.; Mettler, T.; Messerli, G.; Hörtensteiner, S.; Zeeman, S.C. Blocking the Metabolism of Starch Breakdown Products in *Arabidopsis* Leaves Triggers Chloroplast Degradation. *Mol. Plant* **2009**, *2*, 1233–1246. [[CrossRef](#)] [[PubMed](#)]
64. Austin, J.R.; Frost, E.; Vidi, P.-A.; Kessler, F.; Staehelin, L.A. Plastoglobules Are Lipoprotein Subcompartments of the Chloroplast That Are Permanently Coupled to Thylakoid Membranes and Contain Biosynthetic Enzymes. *Plant Cell* **2006**, *18*, 1693–1703. [[CrossRef](#)]

65. Besagni, C.; Kessler, F. A mechanism implicating plastoglobules in thylakoid disassembly during senescence and nitrogen starvation. *Planta* **2013**, *237*, 463–470. [[CrossRef](#)] [[PubMed](#)]
66. Gaude, N.; Bréhélin, C.; Tischendorf, G.; Kessler, F.; Dörmann, P. Nitrogen deficiency in Arabidopsis affects galactolipid composition and gene expression and results in accumulation of fatty acid phytyl esters. *Plant J.* **2007**, *49*, 729–739. [[CrossRef](#)] [[PubMed](#)]
67. Lichtenthaler, H.K. Biosynthesis, accumulation and emission of carotenoids, α -tocopherol, plastoquinone, and isoprene in leaves under high photosynthetic irradiance. *Photosynth. Res.* **2007**, *92*, 163–179. [[CrossRef](#)]